Time-Domain Assessment of the Unstirred Rays in Reverberation Chambers

Guillaume Andrieu[1], Alain Reineix[1]
[1]XLIM Laboratory, University of Limoges, 123 avenue Albert Thomas, 87000 Limoges, France,
guillaume.andrieu@xlim.fr & alain.reineix@xlim.fr

Abstract

This paper present original time-domain results able to quantify the effect of unstirred rays in a reverberation chamber (RC). Although these results are also based on S-parameter measurements between two antennas, these results gives different information in comparison to the well-known frequency domain K-factor [1]. In particular, it is possible to know accurately the time of arrival of the unstirred rays Consequently, they allow one to optimize the position of the emitting antenna for electromagnetic compatibility (EMC) testing and to strengthen the understanding of a RC behaviour in the time domain.

1. Introduction

The assessment of the unstirred rays in RC is a topic of interest over the last years for both EMC and antenna communities. These communities use successfully the K-factor [1-2] to assess the influence of the unstirred rays in a RC. Unfortunately, as it is shown in this paper, this metric is difficult to interpret on a large frequency range which is the case of EMC testing. In this case, the unstirred rays have to be minimized in order to obtain EM field distributions in the working volume tending toward the distributions [3] predicted by the ideal model [4]. This paper presents different time-domain results able to add additional information as the time of arrival of the unstirred rays for instance. In particular, it is shown that the influence of the stirred rays is mainly occurring in the buildup time of the RC [5].

2. Description of the measurements

The S-parameter measurements have been performed between two identical broadband log-periodic antennas (ETS-Lindgren 3148) in the RC of the XLIM laboratory (dimensions : 3.57*2.46*2.46 m) previously optimized at low frequency in a previous paper [6]. The mechanical mode stirrer contains 8 metallic blades and the optimal loading made of 6 pyramidal absorbers is inserted in the RC far from the working volume.
Three configurations have been studied as it is illustrated in Figure 1:

- Configuration #1 : the emitting antenna is oriented toward the receiving antenna;
- Configuration #2 : the emitting antenna is oriented toward the mode stirrer;
- Configuration #3 : the emitting antenna is oriented toward the mode stirrer, an additional metallic plate (dimensions : 100*60cm) is inserted close to the emitting antenna in order to decrease the influence of the unstirred rays.

The receiving antenna is located within the working volume of the RC and oriented in order to catch the maximal intensity of the unstirred rays (the objective being to study the worst case from the receiving antenna point of view). The distance (≈ 1.75 m) between both antennas remains as much as possible unchanged for all the configurations.
The S-parameters between both antennas have been measured from 100 MHz to 1.5 GHz over 4001 frequency samples equally spaced (corresponding in the time-domain to an observation time t_{max} of 2.85 µs with a time-domain iteration Δt=0.71ns). These measurements have been repeated for 50 positions of the mode stirrer (corresponding to a 7.2° rotation angle between two successive positions of the mode stirrer).

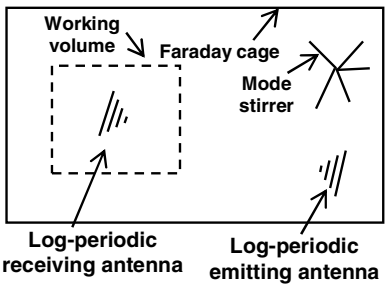

Fig. 1.1 Schematic description of configuration #1 (top view)

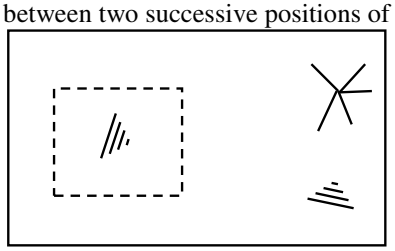

Fig. 1.2 Schematic description of configuration #2 (top view)

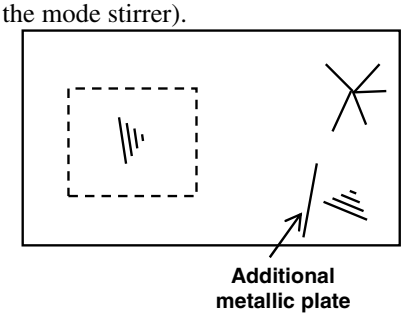

Fig. 1.3 Schematic description of configuration #3 (top view)

978-1-4673-5225-3/14/$31.00 ©2014 IEEE

3. Limits of the K-factor

The K-factor obtained on the whole frequency range considered for all the configurations is plotted in Figure 2. As expected, this figure shows first that the unstirred rays obtained in the first configuration are larger than for the others (as the K-factor is higher for configuration #1). Moreover, the K-factor shows strong local variations over frequency (even if the y-scale is in dB) leading one not be able to differentiate configurations #2 and #3 point of view.

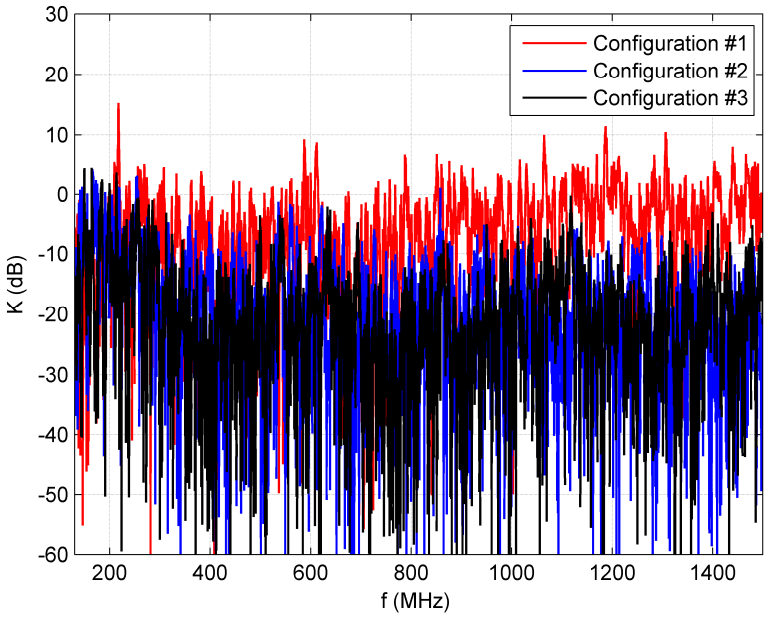

Figure 2 - K-factor (in dB) obtained for the three different configurations

4. Proposed time-domain approaches

The results presented in this paper are obtained first by calculating the impulse response corresponding to each S_{21} parameter measured for each mode stirrer position [5]:

$$h(t,n) = TF^{-1}\left[S_{21}(f,n)\right] \quad (1)$$

where h(t, n) is the impulse response of the RC for the nth position of the mode stirrer which is given by the inverse Fourier transform IFT of S21(f,n).

4.1 Analysis of the power delay profile (PDP)

The (normalized) PDP in a RC is obtained by the following relationship:

$$PDP(t) = \frac{\left\langle h(t,n)^2 \right\rangle}{\max\left[h(t,n)\right]^2} \quad (2)$$

When analyzing this metric in a recent article, Holloway [5], makes the hypothesis that the PDP can be represented by a double-exponential model to take into account the buildup time of the RC. This model seems to be a good approximation in the case of a Rayleigh channel, i.e. without any direct rays. In the presence of unstirred rays of strong magnitude, the PDP has a different shape during the early-time of the RC (see Figure 3.1). This figure shows that the unstirred rays have a strong influence during the early time of the RC. This result can be explained physically by the fact that the more time passes, the greater the chances of bouncing the mode stirrer increases for a particular wave. At this particular moment, this unstirred wave becomes a stirred wave (if we assume that the wave hits the mode stirrer for any position of the mode stirrer). Thus, the value of the PDP (-10dB, -5dB and -3dB for configuration #1, #2 and #3 respectively) obtained when the received power begins to decrease exponentially (at t≈10 µs) can be considered as a good indicator of the influence of the unstirred rays. The introduction of the metallic plate seems to decrease the influence of the stirred rays in the RC.

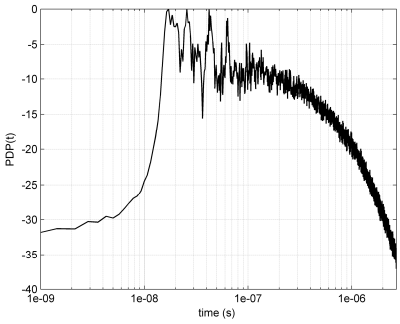

Figure 3.1 - PDP (in a log scale) for configuration #1

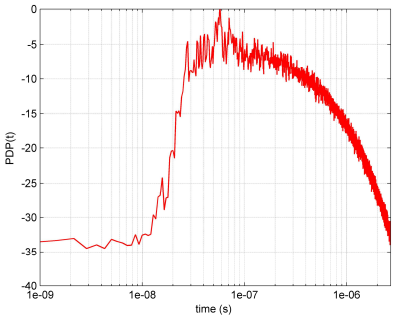

Figure 3.2 - PDP (in a log scale) for configuration #2

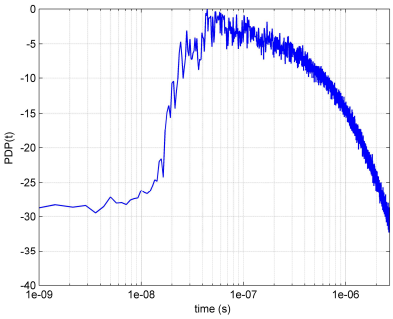

Figure 3.3 - PDP (in a log scale) for configuration #3

4.2 Performing goodness-of-fit (GOF) test according to time

We have also performed Anderson-Darling (AD) GOF test (considered as the most powerful GOF test for analyzing RC data [7] on the n=50 values of h(t,n) obtained for each mode stirrer position at any time considered from t=0s to $t=t_{max}$ (4001 tests have been performed). The aim is to check when the Rayleigh distribution (corresponding to the ideal model) is achieved according to time. Indeed, the hypothesis is when the unstirred rays are predominant, the Rayleigh distribution is rejected. This is confirmed by the results presented in Figure 4.1. It is shown that the tests are mainly rejected during the buildup time (10^{-8} s < t < 10^{-7} s) of the RC for the three different configuration but are massively accepted later for all the configurations. Unfortunately, this interesting result does not allow one to compare the different configurations.

The analysis of the AD statistic (the value compared to the critical value in order to determine if the test is accepted or rejected) according to time gives more information. Figure 4.2 shows first how the AD test is strongly rejected during the buildup time of the RC for configuration #1. The unstirred rays at this moment being highly predominant, h(t) is close to a constant and the Rayleigh distribution is strongly rejected. Indeed, the analysis of the AD statistic allows one to have information at any time on the relative influence of the unstirred rays (with the magnitude of the AD statistic) but also on the time of arrival of each unstirred ray (each corresponding to a peak of the AD statistic). Thus, it is possible to see that the insertion of the metallic plate in configuration #3 leads to delete some unstirred rays during the critical buildup time of the RC.

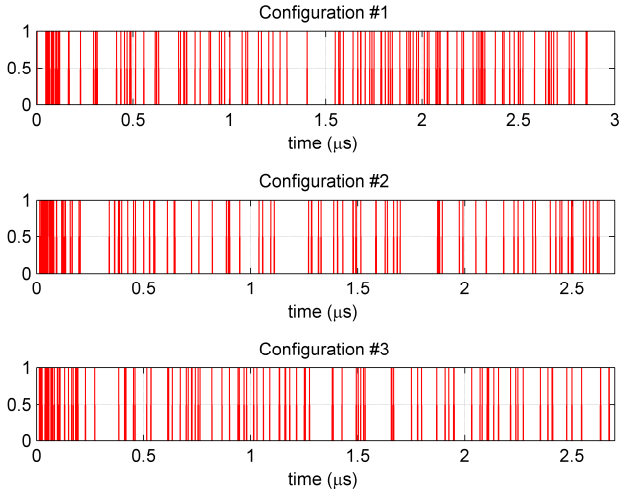

Figure 4.1 - Result of the AD GOF test (1=rejected test, 0=accepted test) obtained according to time for the three configurations

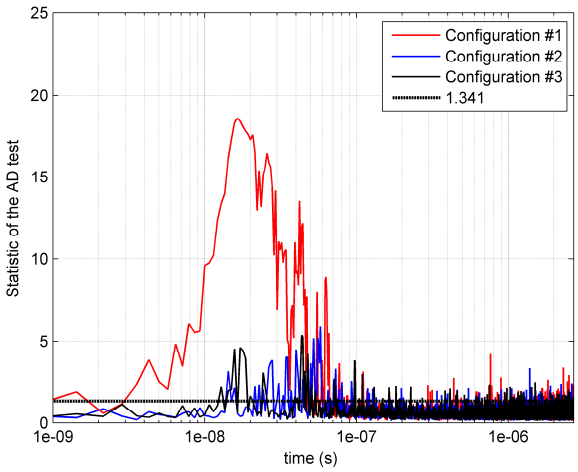

Figure 4.2 - AD statistics obtained according to time for the three configurations

4.3 Analyzing impulse responses

Analyzing directly the impulse responses h(t) obtained for the different mode stirrer positions can also lead to obtain information on the stirred ray influence in a RC. For the three different configurations, we have computed at any time the maximum, the mean and the minimum value of the different values of h(t). Figure 5.1 corresponding to the first configuration clearly shows that during build-up time of the RC, the unstirred rays are predominant as the maximum, the mean and the minimum tends to the same value. Figures 5.1 and 5.2 confirm also the fact that the unstirred rays have weak influence after the buildup time of the RC.

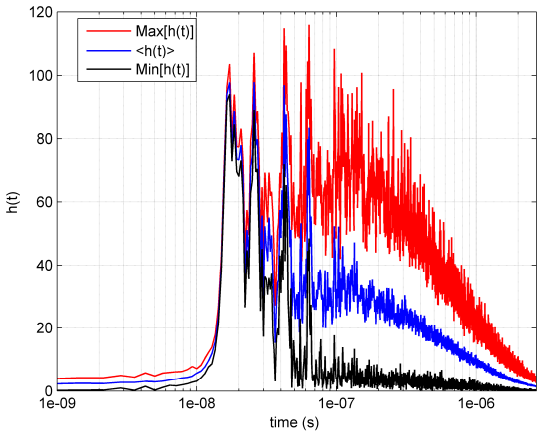

Figure 5.1 - Maximum, mean and minimum of h(t) obtained for the different mode stirrer positions for configuration #1

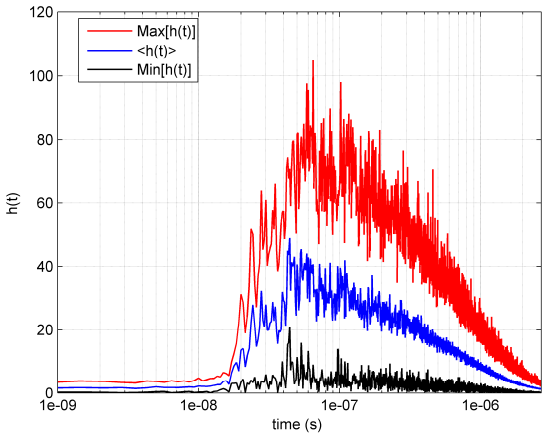

Figure 5.2 - Maximum, mean and minimum of h(t) obtained for the different mode stirrer positions for configuration #3

5. Conclusion

This paper presents useful time-domain results able to highlight the influence of the unstirred rays between two antennas located in a reverberation chamber. These results are complementary to the well-known frequency-domain K-factor metric and gives more reliable information in the case of a broadband source. In particular, it is shown that the unstirred rays have a fundamental influence during the buildup time of the RC. These results can be useful to better understand the behaviour of a RC in the time domain and to optimize the RC [6] for EMC testing as the fact to decrease the amplitude of the unstirred rays has to lead to a better acceptation [3] of the EM field distributions given by the ideal model [4].

6. References

1. C.L. Holloway, D.A. Hill, J.M. Ladbury, P.F. Wilson, G. Koepke, J. Coder, "On the Use of Reverberation Chambers to Simulate a Rician Radio Environment for the Testing of Wireless Devices", *IEEE Trans. on EMC*, vol. 54, no. 11, pp. 3167-3177, Nov. 2006.

2. C. Lemoine, E. Amador, P. Besnier, "On the K-Factor Estimation for Rician Channel Simulated in Reverberation Chamber", *IEEE Trans. on EMC*, vol. 59, no. 3, pp. 1003-1012, Mar. 2011.

3. C. Lemoine, E. Amador, P. Besnier, "Mode-stirring efficiency of reverberation chambers based on Rician K-factor", *Electronic letters*, vol. 47, no. 20, pp 1114-1115, Sep. 2011.

4. D.A. Hill, “Plane wave integral representation for fields in reverberation chambers”, *IEEE Trans. on EMC*, vol. 40, n°3, pp. 209-217, Aug. 1998.

5. C.L. Holloway, H.A. Shah, R.J. Pirkl, K.A. Remley, D.A. Hill, J. Ladbury, "Early Time Behavior in Reverberation Chambers and Its Effect on the Relationships Between Coherence Bandwidth, Chamber Decay Time, RMS Delay Spread, and the Chamber Buildup Time", *IEEE Trans. on EMC*, vol. 54, no. 4, pp. 714-725, Aug. 2012.

6. A. Adardour, G. Andrieu, A. Reineix, "On the Low Frequency Optimization of Reverberation Chambers", *IEEE Trans. on EMC*, accepted for publication, available online in early access.

7. C. Lemoine, P. Besnier, M. Drissi, “Investigation of reverberation chamber measurements through high-power goodness-of-fit tests”, *IEEE Trans. on EMC*, vol. 49, no. 4, pp. 745-755, Nov. 2007.